Numerical simulation of random error in wind profiles for Doppler lidar measurements

Alexander P. Shelekhov[1], Evgeniya A. Shelekhova[1], Alexander V. Starchenko[2], Andrey A. Barth[2], Dmitry A. Belikov[2]

[1] 1 Akademicheskii Ave., 634055 Tomsk, Russian Federation, e-mail: ash@iao.ru,
[2] Tomsk State University, 36 Lenin Ave., Tomsk, 634050, Russia

ABSTRACT

The wind profiles and its random error from the Doppler lidar measurements in the planetary boundary layer (PBL) are simulated numerically. The wind velocity retrievals are performed by minimizing the least-squares fit cost function, which is the difference between the modeled and observed radial wind velocity. The random error in wind profiles is studied using analysis of the Doppler shift of a non-Gaussian random signal. Numerical simulation is based on "e-l" model of atmospheric turbulence and one-dimensional model of the homogeneous PBL, which take into account diurnal variations of meteorological parameters and the turbulent structure of the PBL. In the paper the results of the numerical simulation of profiles of the wind components, its random errors are presented for the case when the atmospheric stratification varies significantly during daytime.

1. DOPPLER LIDAR MEASUREMENT OF WIND PROFILE

For determination of the components of wind vector as a function of height, the least square fit cost function is used [1, 2]

$$L=\sum_{k=0}^{N-1}\left[\overline{u}_r\left(R,\phi_0+k\Delta\phi,\theta\right)-\hat{u}_r\left(R,\phi_0+k\Delta\phi,\theta\right)\right]^2 , \quad (1)$$

$$\hat{u}_r\left(R,\phi,\theta\right)=\hat{U}\sin\phi\cos\theta+\hat{V}\cos\phi\cos\theta , \quad (2)$$

where $\overline{u}_r\left(R,\phi,\theta\right)$ is observed LOS velocity [1], R is distance, ϕ is azimuth angle, θ is elevation angle, $\hat{U}$ and $\hat{V}$ are estimates of wind vector components.

The equations for estimates of wind vector components can be written in the forms [2]

$$\hat{U}=\frac{1}{\left(BC-A^2\right)\cos\theta}\sum_{k=0}^{N-1}\overline{u}_r\left(R,\phi_0+k\Delta\phi,\theta\right)\times$$
$$\times\left[B\sin\left(\phi_0+k\Delta\phi\right)-A\cos\left(\phi_0+k\Delta\phi\right)\right], \quad (3)$$

$$\hat{V}=\frac{1}{\left(BC-A^2\right)\cos\theta}\sum_{k=0}^{N-1}\overline{u}_r\left(R,\phi_0+k\Delta\phi,\theta\right)\times$$
$$\times\left[C\cos\left(\phi_0+k\Delta\phi\right)-A\sin\left(\phi_0+k\Delta\phi\right)\right], \quad (4)$$

$$A=\sum_{k=0}^{N-1}\sin\left(\phi_0+k\Delta\phi\right)\cos\left(\phi_0+k\Delta\phi\right), \quad (5)$$

$$B=\sum_{k=0}^{N-1}\cos^2\left(\phi_0+k\Delta\phi\right), \quad (6)$$

$$C=\sum_{k=0}^{N-1}\sin^2\left(\phi_0+k\Delta\phi\right), \quad (7)$$

where ϕ_0 is the first azimuth angle of the VAD sector scan.

We simulate the observed LOS velocity based on equation of the average radial velocity [2]

$$\overline{u}_r\left(R,\phi,\theta\right)=\frac{1}{N_\phi}\sum_{i=0}^{N_\phi-1}u_r\left(R,\phi_i,\theta\right)\rightarrow$$
$$\rightarrow\frac{1}{\Delta\phi}\int_{\phi-\Delta\phi/2}^{\phi+\Delta\phi/2}u_r\left(R,\phi',\theta\right)d\phi' \quad (8)$$

where $u_r\left(R,\phi,\theta\right)$ is the radial velocity of a single laser pulse.

2. RADIAL VELOCITY OF A SINGLE LASER PULSE

In our study we use model the radial velocity of a single laser pulse, which meets the requirement of the uniform approximation and allows the obtained results to be interpreted correctly [3]. The radial velocity can be written as a sum of a regular part and two fluctuation parts [3, 4]

$$u_r\left(R,\phi,\theta\right)=\left\langle u_r\left(R,\phi,\theta\right)\right\rangle+u'_{ng}\left(R,\phi,\theta\right)+u'_g\left(R,\phi,\theta\right), \quad (9)$$

where

$$\left\langle u_r\left(R,\phi,\theta\right)\right\rangle=U\sin\phi\cos\theta+V\cos\phi\cos\theta \quad (10)$$

is the regular part of the radial velocity,

© Proceedings of the 8th International Symposium on Tropospheric Profiling, ISBN 978-90-6960-233-2
Delft, The Netherlands, October 2009. Editors, A. Apituley, H.W.J. Russchenberg, W.A.A. Monna

$$u'_{ng}(R,\phi,\theta) =$$

$$= \frac{1}{M_s}\sum_{q=0}^{M_s-1}\int\left|p\left(qT_s - 2\frac{R-R_1}{c}\right)\right|^2 u'_r(R_1,\phi,\theta)dR_1 \quad (11)$$

is the non-Gaussian part of fluctuations,

$$u'_g(R,\phi,\theta) = \frac{1}{2kS_0}\sum \omega_i \Delta\hat{S}\left(\omega_i + \Omega_{ng}\right) \quad (12)$$

is the Gaussian part of fluctuations, U and V are components of wind vector, $p(t)$ is temporal profile of laser pulse M_s and T_s are number and time of samples, $\Delta\hat{S}(\omega)$ is spectrum fluctuations of the Doppler lidar signal, S_0 is normalized coefficient, Ω_{ng} is the non-Gaussian part of the Doppler shift.

3. RADIAL VELOCITY OF A SINGLE LASER PULSE

It follows from Eqs. (3) – (9) that $\left\langle\hat{U}\right\rangle = U$ and $\left\langle\hat{V}\right\rangle = V$ if the change in azimuth angle isn't large, i.e. $\Delta\phi \approx 0$. Therefore the expressions for estimation of wind vector components have the form

$$\hat{U} = U + U'_{ng} + U'_g \quad (13)$$

$$\hat{V} = V + V'_{ng} + V'_g \quad (14)$$

where U'_{ng} and V'_{ng} are the non-Gaussian fluctuations of estimation of wind vector components, U'_g and V'_g are the Gaussian fluctuations of estimation of wind vector components.

It is seen that the estimates of $\hat{U}$ and $\hat{V}$ coincide with wind vector components if the Gaussian and non-Gaussian of fluctuations are zero, i.e. $\hat{U} = U$ and $\hat{V} = V$ if $U'_{ng} = U'_g = V'_{ng} = V'_g = 0$. This means that the lidar data may be interpreted as measurements of wind vector components and the variances of $\sigma_U^2 = \left\langle\left(U'_{ng} + U'_g\right)^2\right\rangle$, and $\sigma_V^2 = \left\langle\left(V'_{ng} + V'_g\right)^2\right\rangle$ are the measurements errors.

4. MEASUREMENT ERROR OF COMPONENTS WIND VECTOR

Calculations of the variances of measurement error of wind vector components result in the following expression

$$\sigma_U^2 = \frac{1}{\left(BC - A^2\right)^2\cos^2\theta}\sum_{k''=0}^{N-1}\sum_{k''=0}^{N-1}\left\langle\overline{u}'_{ng}(R,\phi_0 + k'\Delta\phi,\theta)\overline{u}'_{ng}(R,\phi_0 + k''\Delta\phi,\theta)\right\rangle \times$$
$$\times\left[B\sin(\phi_0 + k'\Delta\phi) - A\cos(\phi_0 + k'\Delta\phi)\right]\left[B\sin(\phi_0 + k''\Delta\phi) - A\cos(\phi_0 + k''\Delta\phi)\right] +$$
$$+\frac{B}{\left(BC - A^2\right)\cos^2\theta}\left\{\frac{\sqrt{\pi\left\langle\Delta\omega'^2_d\right\rangle}}{8k^2M_sN_\phi NTS} + \frac{\left\langle\Delta\omega'^2_d\right\rangle}{2k^2M_sN_\phi N}\frac{\mathrm{N}}{\mathrm{S}} + \frac{\pi^2}{12k^2M_sN_\phi NT_s^2}\frac{\mathrm{N}^2}{\mathrm{S}^2}\right\}, \quad (15)$$

$$\sigma_V^2 = \frac{1}{\left(BC - A^2\right)^2\cos^2\theta}\sum_{k''=0}^{N-1}\sum_{k''=0}^{N-1}\left\langle u'_{ng}(R,\phi_0 + k'\Delta\phi,\theta)u'_{ng}(R,\phi_0 + k''\Delta\phi,\theta)\right\rangle \times$$
$$\times\left[C\cos(\phi_0 + k'\Delta\phi) - A\sin(\phi_0 + k'\Delta\phi)\right]\left[C\cos(\phi_0 + k''\Delta\phi) - A\sin(\phi_0 + k''\Delta\phi)\right] +$$
$$+\frac{C}{\left(BC - A^2\right)\cos^2\theta}\left\{\frac{\sqrt{2\pi\left\langle\Delta\omega'^2_d\right\rangle}}{8k^2M_sN_\phi NTS} + \frac{\left\langle\Delta\omega'^2_d\right\rangle}{2k^2M_sN_\phi N}\frac{\mathrm{N}}{\mathrm{S}} + \frac{\pi^2}{12k^2M_sN_\phi NT_s^2}\frac{\mathrm{N}^2}{\mathrm{S}^2}\right\}, \quad (16)$$

$$\left\langle\Delta\omega'^2_d\right\rangle = 1/2\tau_0^2 + \frac{1}{2M_s^2}\sum_{i,j=1}^{M}\int\left|p\left(iT_s - 2\frac{R-R_1}{c}\right)\right|^2\left|p\left(jT_s - 2\frac{R-R_2}{c}\right)\right|^2 D_{\omega'_d}(R_1,R_2;\phi,\theta)dR_1dR_2\,, \quad (17)$$

$$D_{\omega_d'}(R_1,R_2;\phi,\theta)=4k^2\sum_{k,l}\left\langle\left(u_k'(R_1;\phi,\theta)-u_k'(R_2;\phi,\theta)\right)\left(u_l'(R_1;\phi,\theta)-u_l'(R_2;\phi,\theta)\right)\right\rangle \mathrm{n}_k \mathrm{n}_l\,, \tag{18}$$

where S/N is signal-to-noise ratio. It follows from Eqs. (15) and (18) that the Doppler random error in wind profiles depends on the state of the PBL. For simulation of the Doppler random error and wind profiles we use the 1D model of homogeneous PBL and "e-l" – turbulence model [4, 5].

5. MODEL OF PLANETARY BOUNDARY LAYER

For 1D model of homogeneous PBL the equations for average horizontal wind velocity components $U(t,z)$ and $V(t,z)$, average potential temperature $\Theta(t,z)$ and average humidity $Q(t,z)$ have a form [4, 5]

$$\frac{\partial U}{\partial t}=-\langle u'w'\rangle+f\left(V-V_g\right), \tag{19}$$

$$\frac{\partial V}{\partial t}=-\langle v'w'\rangle+f\left(U-U_g\right), \tag{20}$$

$$\frac{\partial \Theta}{\partial t}=-\langle \theta'w'\rangle\,,\ \frac{\partial Q}{\partial t}=-\langle q'w'\rangle\,, \tag{21}$$

where $U_g=-\frac{1}{\rho f}\frac{\partial p}{\partial y}$, $V_g=\frac{1}{\rho f}\frac{\partial p}{\partial x}$ is the components of the geostrophic wind, t is time, z is the vertical coordinate, ρ is the density, p is the pressure, $f=2\Omega\sin\psi$ is the Coriolis parameter, ψ - is the geographic latitude, Ω is the angular velocity of the Earth revolution. For describing the turbulence that essentially influences the structure of PBL, we use "e-l" – the atmospheric turbulence model [4, 5].

6. MODEL OF ATMOSPHERIC TURBULENCE

The equation for "e-l" – turbulence model can be written in the form [4, 5]

$$\frac{\partial e}{\partial t}=-\langle u'w'\rangle\frac{\partial U}{\partial z}-\langle v'w'\rangle\frac{\partial V}{\partial z}+\frac{g}{\Theta}\langle\theta'w'\rangle+\frac{\partial}{\partial z}\left(\sigma_e\sqrt{el}\,\frac{\partial e}{\partial z}\right)-\frac{C_De^{3/2}}{l} \tag{22}$$

$$\frac{\partial l}{\partial t}=C_{L1}\left(-\langle u'w'\rangle\frac{\partial U}{\partial z}-\langle v'w'\rangle\frac{\partial V}{\partial z}+\frac{g}{\Theta}\langle\theta'w'\rangle\right)\frac{l}{e}+\frac{\partial}{\partial z}\left(\sigma_e\sqrt{el}\,\frac{\partial l}{\partial z}\right)+C_{L2}\sqrt{e}\left[1-\left(\frac{l}{\kappa z}\right)^2\right] \tag{23}$$

$$\frac{\partial\langle\theta^2\rangle}{\partial t}=\frac{\partial}{\partial z}\left(C_\theta\sqrt{el}\,\frac{\partial\langle\theta^2\rangle}{\partial z}\right)-2\langle w\theta\rangle\frac{\partial\Theta}{\partial z}-2\frac{\langle\theta^2\rangle}{C_\theta\tau} \tag{24}$$

$$\varepsilon=\frac{C_De^{3/2}}{l}\,,\ \langle u'w'\rangle=-F_m\sqrt{el}\,\frac{\partial U}{\partial z}\,,\ \langle v'w'\rangle=-F_m\sqrt{el}\,\frac{\partial V}{\partial z}\,,\ \langle\theta'w'\rangle=-F_h\sqrt{el}\,\frac{\partial\Theta}{\partial z}\,, \tag{25}$$

where $e=\left(\frac{1}{2}\langle u'^2\rangle+\langle v'^2\rangle+\langle w'^2\rangle\right)$ is the kinetic energy of turbulence; l is the scale of turbulence, $\langle\theta^2\rangle$ is the turbulent temperature pulsations, ε - is the energy dissipation rate, $\sigma_e=0.54$, $C_{L1}=-0.12$, $C_{L2}=0.2$, $C_D=0.19$, $\kappa=0.4$, F_m and F_h are the function of local turbulent characteristics [4, 5].

7. RESULTS OF NUMERICAL SIMULATION

Figures 1 and 2 present the results of numerical simulation of profiles for components of wind vector. The initial meteorological data, required for short-prediction, were taken from archive of website of the University of Wyoming (www.weather.uwyo.edu). Measurement data on geostrophic wind, temperature, humidity, and other atmospheric parameters were obtained from weather stations CNK, CNU, SLN, TOP (abbreviated). The basic station was TOP. The results of numerical simulation are obtained for the CASES-99 field site near Leon, Kansas and for October 6, 1999.

It follows from numerical simulation that the components of wind vector and also turbulent kinetic energy and length scale strongly change during the day. For example, it is clear from figures 1 and 2 that the strong wind is observed. Where turbulence changes sharply ($t(z)$=4 h, $t(z)$=15 h, and $t(z)$=20 h) the shear in the wind appears at the atmosphere.

Figure 3 shows the results of numerical simulation of the variances of measurement error of wind vector components in the case of $M_s=10$, $N_\phi=10$, $N=100$, and $\mathrm{S/N}=1$ for $z=100$ m.

The variances of measurement error of wind vector components depend on state of atmospheric turbulence and lidar parameters. It follows from figure 3 that the measurement error increases with increase of the energy of turbulence. In our case the measurement error is defined by the Gaussian fluctuations of the Doppler shift for weak turbulence. The measurement error depends on the non-Gaussian fluctuations of the Doppler shift for strong turbulence.

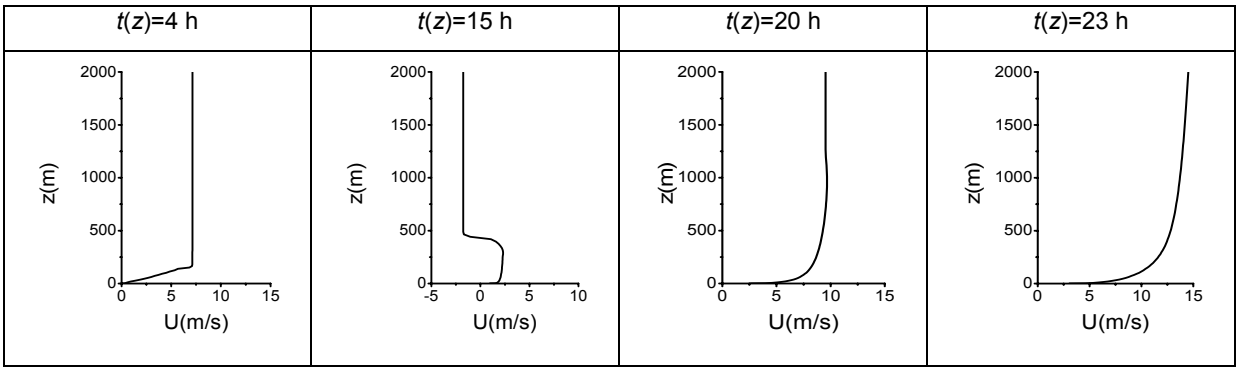

Figure 1. *Profiles of $U(z)$ component of wind vector during the day, Oct. 06, 1999.*

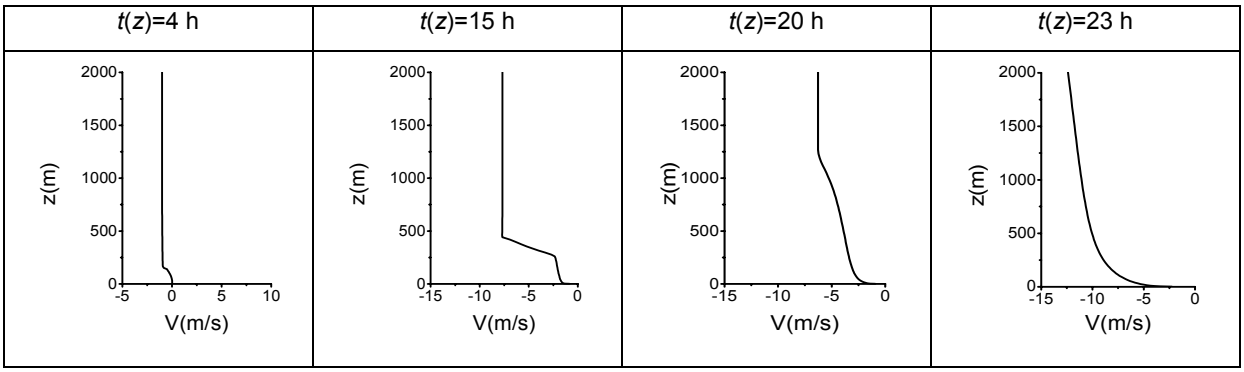

Figure 2. *Profiles of $V(z)$ component of wind vector during the day, Oct. 06, 1999.*

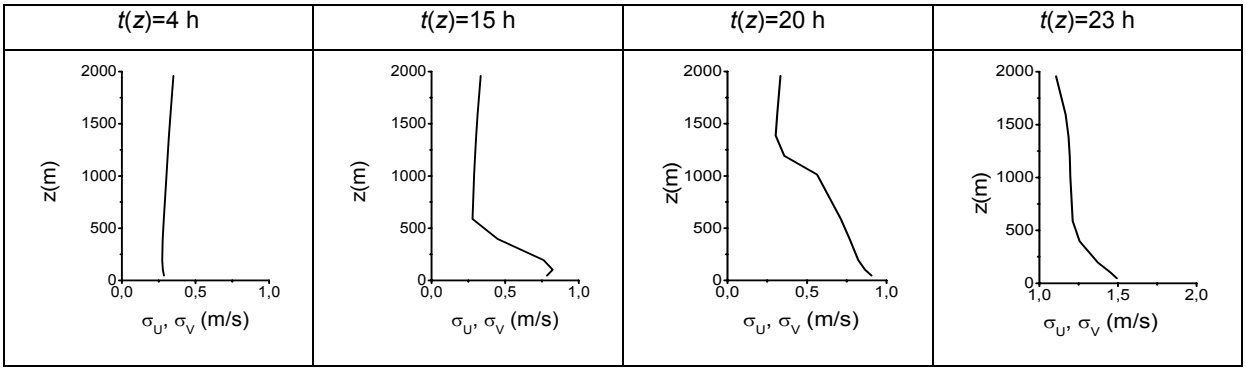

Figure 3. *Profile of measurement error during the day, Oct. 06, 1999.*

REFERENCES

[1] Brewer A. Tucker S. Hardesty M. 2008: Evaluation of motion stabilization system using random errors in wind profiles measured by a ship-based, scanning Doppler lidar, *Reviewed and revised papers presented at the 24th International Laser Radar Conference. 23-27 June 2008, Boulder, Colorado,* **1**, pp. 235-238.

[2] Frehlich R., Mellier Y., Jensen M., Balsley B, Sharman R. 2006: Measurement of boundary layer profiles in an urban environment, *J. of Appl. Meteorology and Climatology,* **45**, № 6, pp. 821-837.

[3] Shelekhov A.P. 1997: Uniform approximation in application to small perturbation methods in problems of statistical analysis of Doppler measurements, *J. Atmos. Oceanic Opt.*, **10**, No.10, pp. 771-776.

[4] Shelekhov A.P., Shelekhova E.A., Belikov D.A., and Starchenko A.V. 2008: Numerical model for prediction of the Doppler measurement accuracy in the atmospheric boundary layer, *J. Atmos. Oceanic Opt.*, **21**, No. 9, pp. 709-714.

[5] Starchenko A. V., Belikov D. A. 2003: A numerical model for real-time monitoring of urban air quality, *J. Atmos. Ocean Opt.*, **16**, No. 7, pp. 608-615.